J Wood Sci (2011) 57:114–118
DOI 10.1007/s10086-010-1154-x

ORIGINAL ARTICLE

Hiroaki Nagai · Koji Murata · Takato Nakano

Strain analysis of lumber containing a knot during tensile failure

Received: April 12, 2010 / Accepted: August 31, 2010 / Published online: December 30, 2010

Abstract We analyzed the strain distribution of lumber containing a knot under a tensile load. The local tensile strain near the knot was measured using the digital image correlation method. Fracture often initiated near the knot where the fiber orientation changed in a three-dimensional manner. The fiber direction in this zone was different from that in the clear part, coinciding with the thickness direction and not with the longitudinal direction of the specimen. Our results disagree with those of previous models that assumed the longitudinal direction of lumber as the direction of crack propagation. Strain analysis showed that a nonlinear region existed around the knot just before ultimate fracture occurred. The results indicated that nonlinear characterization is necessary to determine the failure mechanism of lumber containing a knot, despite the brittleness fracture at the macroscopic scale.

Key words Strain distribution analysis · Knot · Digital image correlation

Introduction

Knots cause strength reduction in lumber; therefore, many studies on evaluation of knots[1,2] have been performed. The strain/stress distribution in lumber with knots has been demonstrated by applying measurements with brittle paints,[3] photoelasticity,[4] or finite element method (FEM) analyses.[5–8] The actual mechanical behavior in the vicinity of a knot, however, is very complicated and is not yet fully understood. In this study, the strain distribution in the vicinity of a knot is obtained by the digital image correlation (DIC) method, which is one of the techniques for strain measurement using digital images.[9,10] DIC is effective for observing subsequent strain distributions continuously. For several years, DIC has been applied to research the heterogeneous characteristics of wood resulting from the presence of earlywood and latewood[11] and the strain distribution in lumber containing a knot under a bending load.[12]

In order to estimate the ultimate strength of lumber with knots, several fracture models have been proposed. Zandbergs and Smith[6] simulated the progressive failure process of tensile fracture. Initial failure (crack initiation) was predicted using the maximum stress theory, and subsequent crack propagation was studied using linear fracture mechanics. They considered the longitudinal direction of lumber to be the direction of crack propagation. Cramer and Fohrell[7] introduced this model to dive angles (out-of-plane grain angles) for describing the three-dimensional orientation of wood fibers.

We reviewed the fracture models proposed in earlier studies, since it is unlikely that these models reflect fracture behavior under real conditions. The purposes of this study were to observe the strain distribution near a knot and to reveal the failure mechanism of lumber with a knot.

Experimental

Materials

In all, ten lumber specimens of Japanese cedar (*Cryptomeria japonica*) from the Koka region of Shiga Prefecture were used (Table 1). Knot position was not considered in this study, since the bending moment derived from the elastic asymmetry when a knot is located at the edge affects the nominal tensile strength of lumber but not the local strain value, which we focus on here. Except for one clear specimen, all specimens contained a single knot that was expected to cause fracture. In order to investigate various types of knots (e.g., round, spike, encased, and intergrown), flat-sawn and quarter-sawn specimens were used. The specimen dimensions were 50 mm thick × 105 mm wide × 2400 mm long. The average density of the specimens was 381 kg/m^3. A random dot pattern was generated on the surface of the

H. Nagai (✉) · K. Murata · T. Nakano
Division of Forest and Biomaterials Science, Graduate School of Agriculture, Kyoto University, Kitashirakawa, Oiwake-cho, Sakyo-ku, Kyoto 606-8502, Japan
Tel. +81-75-753-6236; Fax +81-75-753-6300
e-mail: nagai@h1sparc1.kais.kyoto-u.ac.jp

Table 1. Properties of specimens

Specimen	Knot position	Knot type	Knot ratio (%)	Density (kg/m^3)	Tensile strength (MPa)	Failure position
1 (Knotted)	Edge	Encased / round	26.9	356	21.6	Knot
2 (Knotted)	Center	Encased / round	17.0	363	–	Grip
3 (Knotted)	Edge	Intergrown / round	35.5	386	19.0	Knot
4 (Knotted)	Edge	Encased / round	19.5	360	15.4	Knot
5 (Knotted)	Edge	Encased / spike	36.3	400	–	Grip
6 (Knotted)	Edge	Intergrown / round	36.5	391	14.3	Knot
7 (Knotted)	Center	Intergrown / spike	20.8	347	–	Grip
8 (Knotted)	Edge	Encased / spike	57.7	356	22.6	Knot
9 (Knotted)	Center	Intergrown / round	27.6	349	23.3	Knot
10 (Clear)	–	–	0	318	41.1	Not grip

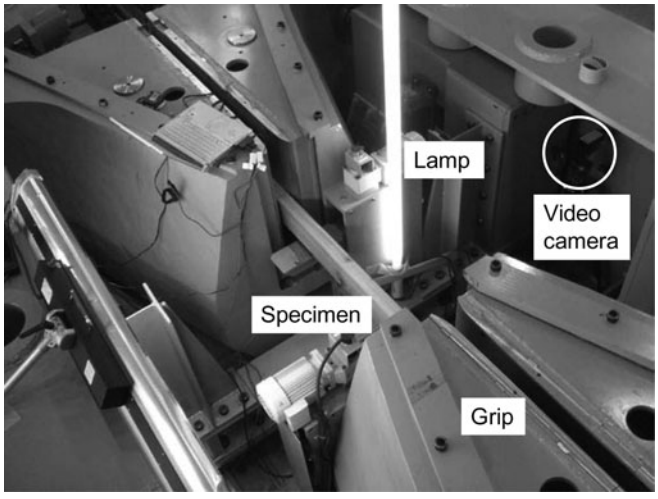

Fig. 1. Tensile test configuration

specimen by spraying it with black water-soluble paint using an airbrush in order to calculate the strain using DIC.

Testing method

The specimens were tested on a tensile testing machine for structural lumber (Maekawa HZS-200-LB4). Details of the test configuration are shown in Fig. 1. The velocity of the crosshead was 8 mm/min and the length between the grips was 1000 mm. In the tension test, the apparent elongation of the specimens was measured as the displacement between the grips, and the deformation of the specimen was continuously recorded using two digital video cameras (Sony XCD-SX910). The cameras were placed symmetrically equidistant from the specimen surfaces on either side of the specimen in order to acquire images of both sides. The images were captured at intervals of 0.532 s with a digital image capture system (Library; Digital Capture). The frame size of the monochrome digital images was 1280×960 pixels, and their resolution was approximately 0.16 mm/pixel.

Strain measurement using DIC

DIC was used to measure the deformation and calculate the strain in each specimen. In-house software was used for DIC analysis in this study, and it had an accuracy of ±500 microstrains in terms of the standard deviation.[10,13] A DIC analysis field consisting of aligned elements was established at the region where rupture would occur. The strain in an element was calculated by measuring the displacement vectors of the four nodes that constitute the element.

Results and discussion

Tension test

Three of the nine knotted specimens that exhibited rupture in the grip region were excluded from the analysis. The mean tensile strength was 22.5 N/mm^2, and all the specimens satisfied the criterion of the standard strength of Japanese cedar (according to the Ministry of Land, Infrastructure, Transport and Tourism, Government of Japan, Ministerial announcement No. 1024,[14] which is 13.5 N/mm^2). In some specimens, the load increased after visible crack initiation at the surface of the specimen.

Six of the nine knotted specimens ruptured in the vicinity of the knot under observation. All the cracks initiated at a transition zone between the knot and the clear part. According to Shigo,[15] the fibers are arranged in a complex pattern in this transition zone. Except for one specimen, fracture occurred where the fiber orientation changed in a three-dimensional manner. In the transition zone, the fiber orientation is not in the longitudinal direction or the width direction, but in the thickness direction of the specimen (Fig. 2). The transition zone surface was therefore assumed to be a transverse plane (R-T). In other words, the crack propagated along the thickness direction of the specimen, and thus remains unexplained in two-dimensional failure models of lumber with a knot.[6,7]

Strain analysis

Large strains were concentrated near knots. However, there was no marked correlation between the tensile strength and the maximum strain in the horizontal/vertical directions of the captured image. The reason for this was considered to be that the crack propagated in neither in the horizontal nor the vertical direction. Therefore, we replaced the specimen coordinate system with another coordinate system that

is defined as the direction of the crack and the direction perpendicular to it. Figure 3 shows the relationship between the maximum normal strain and the tensile strength in the new coordinate system. The maximum strain perpendicular to the direction of crack propagation was larger than that along the direction of crack propagation, as is well known, and this is consistent with inferences based on observation of the fracture surface. For most samples, the strain perpendicular to the direction of crack propagation reached a value of almost 1.5%. The proportional limit on the stress–strain curve obtained by Miyauchi and Murata[16] was approximately 1% strain. When a localization zone of strain above the proportional limit is regarded as a nonlinear zone, apparent nonlinear behavior was observed near knots just before fracture occurred. We believe this apparent nonlinear behavior to result from the combination of elastic deformation and local microscopic failures. The cracks in four of the specimens that led to ultimate failure propagated diagonally, while those in the remaining two specimens propagated at right angles to the loading direction (Fig. 4). The maximum shear strain was roughly 2%–3% for edge cracks that propagated obliquely with respect to the loading direction, unlike the case of crack propagation perpendicular to the loading direction (Fig. 4). It is considered that these different modes of crack propagation were caused by the positional relation between the crack initiation point and the knot, which has higher density than the surroundings.

The strain profiles of samples in which an edge crack propagated perpendicular to the loading direction were analyzed in detail in order to determine the failure process. An example of the strain profile in the width direction of the specimen at a tension load of 120 kN is shown in Fig. 5. In this specimen, fracture initiated at the bottom edge since the strain perpendicular to crack was concentrated by the edge knot. Figure 6 shows the change in the edge strain profile with increasing load. Profiles are shown for loads of

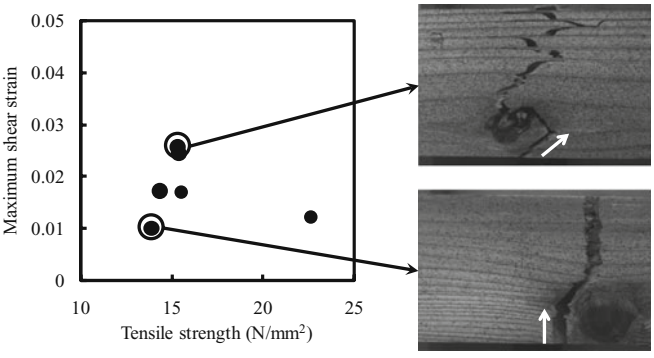

Fig. 4. Relationship between fracture morphology and maximum shear strain in the transformed coordinate system

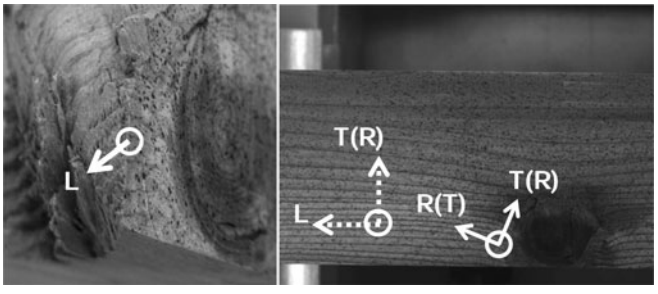

Fig. 2. Direction of fiber orientation in the transition zone (*solid lines*) and clear part of lumber (*dashed line*)

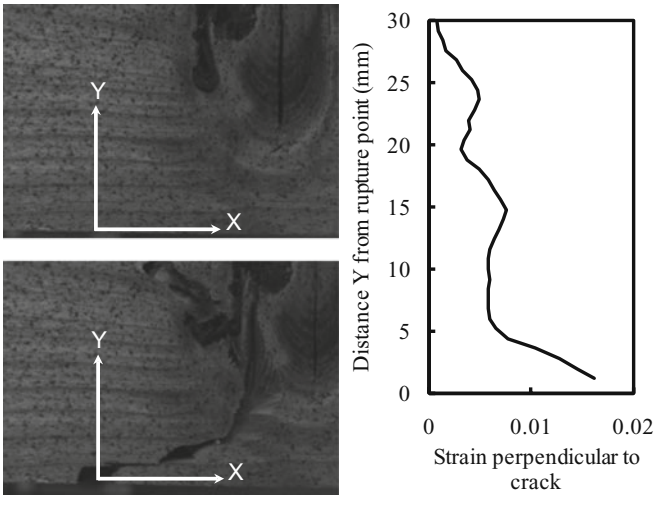

Fig. 5. Strain profile in the width direction of specimen No. 8 at a tension load of 120 kN. Fracture initiated at the bottom edge and propagated in the Y direction

Fig. 3. Maximum normal strain and tensile strength in the transformed coordinate system for the six samples that failed near the knot. The same symbols represent the same specimens

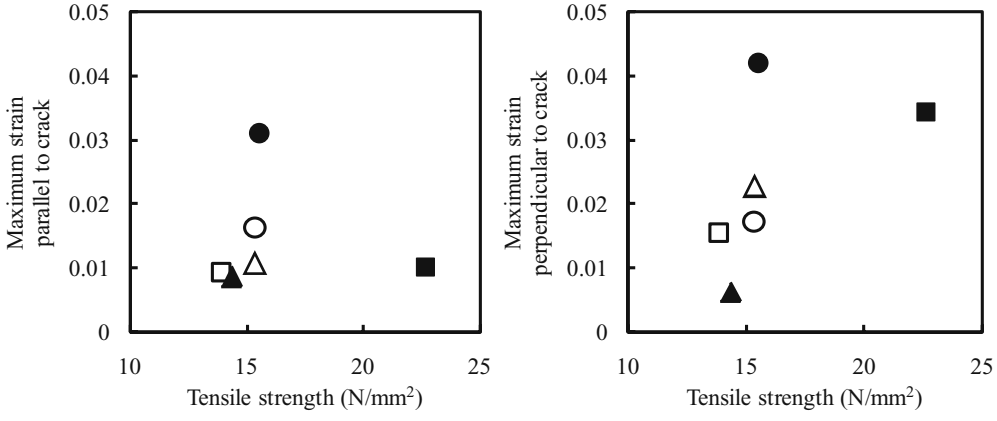

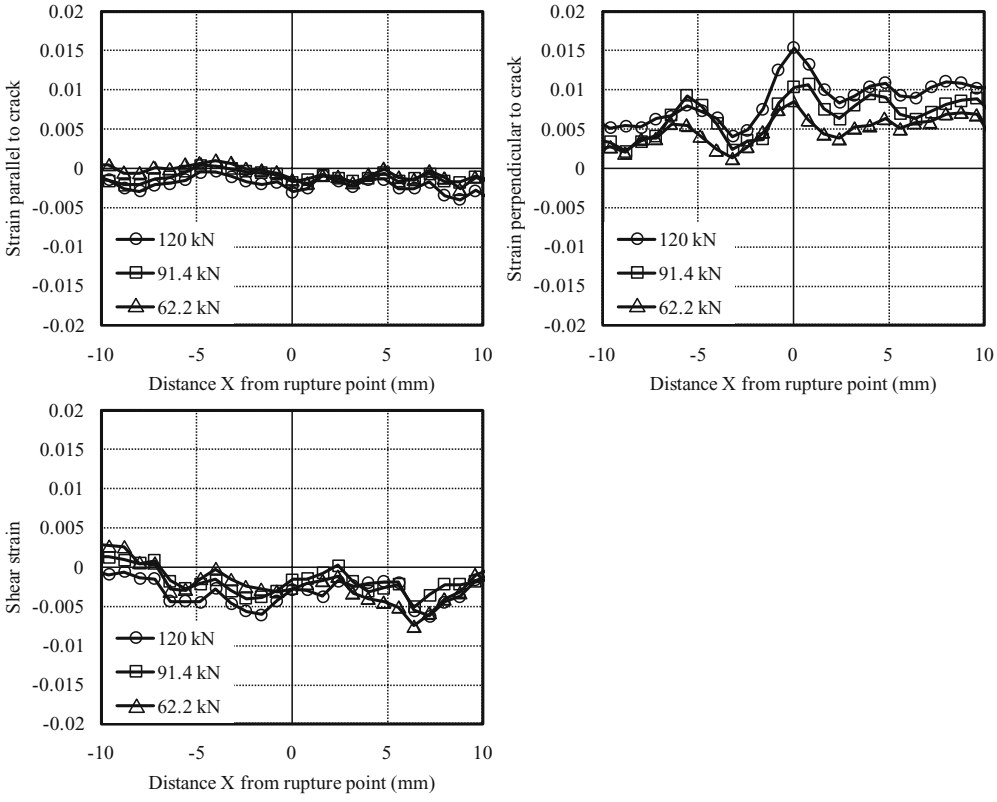

Fig. 6. Change of edge strain profile with increasing load (refer to Fig. 5 for the X direction). Profiles are shown for loads of 62.2, 91.4, and 120 kN

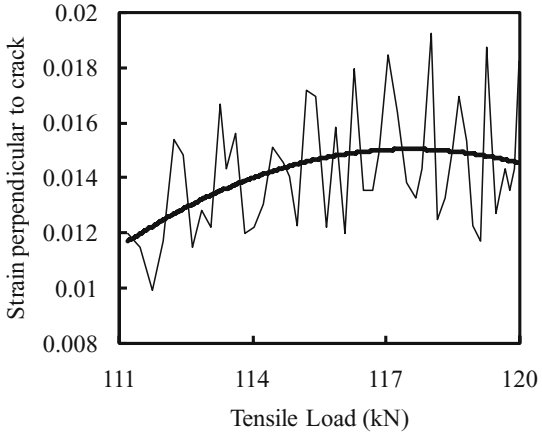

Fig. 7. Strain just before ultimate fracture in the element in which the fracture would occur; the failure load was 120.1 kN

62.2, 91.4, and 120 kN. Since the Y strain (parallel to crack) was larger than the X strain (perpendicular to crack) and the shear strain, loading perpendicular to the grain is likely to induce tensile fractures. With increasing load, the Y strain profile showed strain concentrated at the region where the rupture would occur. The maximum Y strain was 1.6%. Figure 7 shows the strain at the rupture element just before fracture occurred (the failure load was 120.1 kN). The plotted smoothed curve was approximated by a quadratic equation using Microsoft Excel. The image resolution was not high (0.16 mm/pixel) since the entire width of the lumber specimen was captured. It was observed that the strain tends to increase with large oscillations around the mean value, although the measured strain data contained noise that occurs during the measuring process, caused, for example, by glittering on the lumen surface of tracheids, electric signal noise, or interpolation error during digital signal processing. This issue represents the nonlinearity in the stress/strain relationship in the region near the knot.

Since a nonlinear zone was observed near knots just before fracture, we believe that nonlinear characterization is necessary to determine the failure mechanism of lumber containing knots. According to Vasic et al.,[17] the fracture process zone (FPZ) located around a crack tip has been characterized in terms of the failure mechanisms of wood. It is known that strain-softening behavior occurs in the FPZ. When an undamaged specimen is subjected to tensile stress, it stores elastic strain energy. At the maximum stress, the FPZ begins to grow as strain softening occurs. We believe that strain-softening behavior principally results from local brittle failure, and the failure releases elastic strain in the surrounding area. With regard to strain distribution, it is expected that the release of elastic energy would increase the strain in the FPZ and decrease the strain in the periphery of the FPZ just below the failure load. Figure 8 shows the transition of the strain profiles at the rupture element and at an adjacent element. The strain at the rupture element in the stress direction decreased just before fracture. The decrease in the periphery of the FPZ was confirmed, although the increase of strain in the FPZ was difficult to observe in this study. However, it is at present not possible

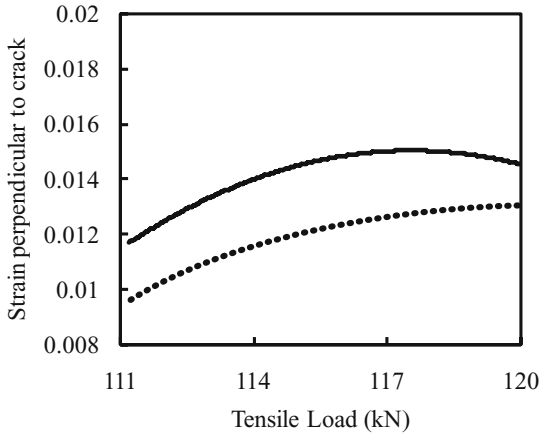

Fig. 8. Transition of strain profiles at the rupture element (*solid line*) and at an adjacent element in the stress direction (*dotted line*)

to arrive at a definite conclusion since the measured strain contained a large amount of noise and was based on low-resolution images. It is expected that observations at a higher resolution will solve this problem.

Conclusions

We conducted tension tests and observed the strain distributions during these tests in order to determine the fracture mechanism of lumber containing a knot. The local tensile strain near the knots was measured using digital image correlation. Tensile fracture initiated near knots where the fiber orientation changed in a three-dimensional manner. The fiber direction in this zone was different from that in the clear part, and the fiber dived into the inside of the specimen. The strain distribution profiles showed the presence of a nonlinear region around knots just before ultimate fracture occurred. In this study, the fracture process zone that appeared at the crack tip was used to study the nonlinear wood behavior. It seemed that in the same way as a clear specimen, lumber containing knots exhibits strain-softening behavior during tensile fracture.

Acknowledgments This research was supported by a Grant-in-Aid (No. 20083182) from the Ministry of Education, Culture, Sports, Science and Technology of Japan. The authors are grateful to the members of the Laboratory of Engineered Timber and Joints, Forestry and Forest Products Research Institute, for their support during the experiments.

References

1. Oh JK, Shim K, Kim KM, Lee JJ (2009) Quantification of knots in dimension lumber using a single-pass X-ray radiation. J Wood Sci 55:264–272
2. Oh JK, Kim KM, Lee JJ (2010) Use of adjacent knot data in predicting bending strength of dimension lumber by X-ray. Wood Fiber Sci 42:10–20
3. Sasaki H, Maku T (1962) On the strain distribution and failure of wood plates with a round knot under tensile load (in Japanese). Wood Res 28:1–23
4. Takahashi A (1966) Strain determination of wood by using photoelastic coating technique VI – On the strain distribution of board with a loose knot subjected to tensile load (in Japanese). Mokuzai Gakkaishi 12:63–66
5. Cramer SM, Goodman JR (1983) Model for stress analysis and strength prediction of lumber. Wood Fiber Sci 15:338–349
6. Zandbergs JG, Smith FW (1988) Finite element fracture prediction for wood with knots and cross grain. Wood Fiber Sci 20:97–106
7. Cramer SM, Fohrell WB (1990) Method for simulating tension performance of lumber members. J Struct Eng 116:2729–2746
8. Itagaki N, Mihashi H, Ninomiya S, Yoshida N, Esashi T (1999) Influence of knots on tensile strength of sugi lamina (in Japanese). Mokuzai Gakkaishi 45:367–374
9. Jeong GY, Zink-Sharp A, Hindman DP (2009) Tensile properties of earlywood and latewood from loblolly pine (*Pinus taeda*) using digital image correlation. Wood Fiber Sci 41:51–63
10. Murata K, Masuda M, Ukyo S (2005) Analysis of strain distribution of wood using digital image correlation method – Four-point bending test of timber including knots (in Japanese). Trans Vis Soc Jpn 25:267–273
11. Ljungdahl J, Berglund LA, Burman M (2006) Transverse anisotropy of compressive failure in European oak – A digital speckle photography study. Holzforschung 60:190–195
12. Shipsha A, Berglund LA (2007) Shear coupling effects on stress and strain distributions in wood subjected to transverse compression. Compos Sci Tech 67:1362–1369
13. Murata K, Masuda M, Ichimaru M (1999) Analysis of radial compression behavior of wood using digital image correlation method (in Japanese). Mokuzai Gakkaishi 45:375–381
14. Ministry of Land, Infrastructure, Transport and Tourism (2001) Ministerial announcement No. 1024. http:www.mlit.go.jp/pubcom/07/pubcomt132/06.pdf (in Japanese)
15. Shigo AL (1985) How trees are attached to trunks. Can J Bot 63:1391–1401
16. Miyauchi K, Murata K (2007) Strain-softening behavior of wood under tension perpendicular to the grain. J Wood Sci 53:463–469
17. Vasic S, Smith I, Landis E (2002) Fracture zone characterization – micro-mechanical study. Wood Fiber Sci 34:42–56